
CALCULATIONS OF NEUTRON FLUXES AND ISOTOPE CONVERSION RATES IN A THORIUM-FUELLED MYRRHA REACTOR, USING GEANT4 AND MCNPX

Asiya Rummana

University of Technology and Applied Sciences - Ibra, Oman

E-mail: Asiya.Rumana@gmail.com

Roger John Barlow

The University of Huddersfield, Huddersfield, UK

E-mail: R.Barlow@hud.ac.uk

Syed Mohammad Saad

University of Technology and Applied Sciences - Ibra, Oman

E-mail: syedsaad@ict.edu.om

ABSTRACT

Neutronics calculations have been performed of the MYRRHA ADS Reactor with a thorium-based fuel mixture, using the simulation programs MCNPX [1] and Geant4 [2]. Thorium is often considered for ADS systems, and this is the first evaluation of the possibilities for thorium based fuels using a reactor design which has been developed in detail. It also extends the application of the widely-used Geant4 program to the geometry of MYRRHA and to thorium. An asymptotic $^{232}\text{Th}/^{233}\text{U}$ mixture is considered, together with the standard MOX fuel and a possible $^{232}\text{Th}/\text{MOX}$ starter. Neutron fluxes and spectra are calculated at several regions in the core: fuel cells, IPS cells and the two (Mo and Ac) isotope production cells. These are then used for simple calculations of the fuel evolution and of the potential for the incineration of minor actinide waste. Results from the two programs agree and support each other and show that the thorium fuel is viable, and has good evolution/breeding properties, and that minor actinide incineration, though it will not take place on a significant scale, will be demonstrable.

1 Introduction

1.1 Accelerator Driven Subcritical Reactors

Accelerator Driven Subcritical Reactor (ADSR) systems have been much discussed since their original proposal by Bowman [3] and Rubbia [4]. A core containing fissile isotopes is exposed to spallation neutrons from a high current particle beam (usually protons). k_{eff} , the criticality of the core is below 1 – typical designs have values in the range 0.90 to 0.98 – which provides a multiplication factor $\frac{1}{1-k_{\text{eff}}}$ (hence the name "energy amplifier") but never sends the system critical. A full account is given in [5] and [6].

As well as their enhanced safety such systems also have the possibility to convert long-lived minor actinide (MA) waste to short-lived fission products, particularly when a fast neutron spectrum and the thorium fuel cycle are used, for four principal reasons.

- Neutron fluxes can be much higher than is possible in critical reactors: as discussed by Bowman [3] they can readily produce fluxes of $\sim 10^{16}\text{ n/cm}^2\text{ s}$, as opposed to $\sim 10^{14}$ for a power reactor or $\sim 10^{15}$ for a 'high flux' reactor, as to the lack of heating from fissions means high flux can be attained at low thermal power, and safely below criticality.

- For fast neutrons, the ratio of fission cross sections to absorption cross sections is higher than in the classical thermal (water based) reactor situation.
- The production of further MA nuclei from ^{232}Th is less than for ^{238}U as more absorptions are needed and the cross sections are smaller.
- Variations in k_{eff} due to variations in reactivity do not have to be exactly compensated for.

Partitioning and transmutation in association with accelerator driven systems and in combination with geological disposal can provide a solution for the nuclear waste management problem [7]. ADSRs can burn not only their own minor actinides but also those produced by light-water reactors.

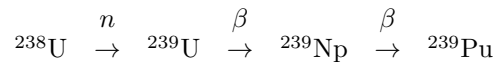
Many relevant experiments have been performed: the MUSE program at Cadarache, GUINEVERE, Yalina at Sosny, and HYPER at Seoul National University[8], culminating in the exposure of the CUCA critical assembly to a beam of protons, in which fission neutrons were observed[9], albeit with a current of nanoamps rather than that milliamps that will be needed for a commercial ADSR system.

1.2 ADS systems and thorium

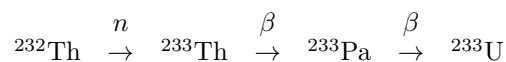
ADSR with thorium fuel has gained large scale interest worldwide in the past two decades for energy production and waste transmutation, following the ‘Energy Amplifier’ proposal of Rubbia [4]. Although ADSR are capable of burning any type of fuel, the choice of thorium provides the benefit of low radiotoxicity and proliferation resistance [10].

For the disposal of high activity nuclear waste, either the spent fuel can be sent for direct disposal (open cycle) or it can be reprocessed to extract transuranic and fission products (closed fuel cycle). The extracted species can then be transmuted into less radiotoxic or short-lived products. Comparisons of open fuel cycle, uranium-plutonium closed cycle and thorium-uranium closed cycle [5] show that closed fuel cycles produced significantly less radiotoxicity than open ones, and that thorium-uranium cycle has about two orders of magnitude lower radiotoxicity, for the first thousand years.

The thorium fuel cycle uses thorium as a fertile seed rather than ^{238}U . Natural thorium (^{232}Th) does not contain any fissile material (unlike natural uranium which contains 0.7% fissile ^{235}U). It cannot be enriched in itself to produce materials of weapons grade so it poses a lower proliferation risk. Thorium can be combined with fissile isotopes (^{235}U or ^{239}Pu) in nuclear reactors for conversion to the fissile ^{233}U . The analogue of the familiar uranium breeding chain which creates fissile ^{239}Pu



is



which produces fissile ^{233}U . These chains are similar, the biggest difference being that the intermediate ^{233}Pa protactinium isotope has a half life of 27 days, much longer than the 2.4 days of the analogous ^{239}Np .

1.3 Minor Actinides

The Minor Actinides (MA) are a major problem for radioactive waste. These are the transuranic elements neptunium (Np), americium (Am) and curium (Cm) which are generated by a combination of successive neutron capture and radioactive decays in a fission reactor. Although they are only few percent of the spent fuel, they are the most problematic part of the nuclear waste as they impose a long term environmental burden of their geological storage. They are highly radio toxic and their half - lives are up to millions of years. If the spent nuclear fuel is not reprocessed it must be treated as High level waste (HLW), and the cost and risk of storing this nuclear waste for a long time cannot be neglected [8].

Minor actinides can be destroyed by transmutation: the process of irradiating them in a high intensity neutron flux in order to decrease the long term radiotoxicity of the spent nuclear fuel. However the production of the neutron flux requires further fissions, and calculations are needed to decide whether the MA component destroyed is outweighed by the additional MA component generated.

Transmutation can occur when the minor actinides are fissioned with a single neutron interaction (direct) or through neutron capture(s) followed by fission (indirect). Since the reaction cross section for both direct and indirect fission

tends to be very low, for effective transmutation the neutron flux should be high and the irradiation time should be long [11].

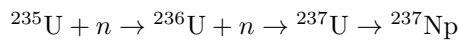
Factors making a particular minor actinide a suitable candidate for transmutation are:

1. Long lifetime
2. High production level
3. Neutron emission and decay heat in the final repository.

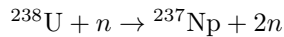
Considering the three elements in turn.

Neptunium (the predominant isotope is ^{237}Np) is considered as secondary candidate for transmutation. It does not contribute to the decay heat output [11]. ^{237}Np is a very long lived nucleide with a half - life of 2.144 million years. The production routes of ^{237}Np are:

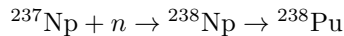
a) Two steps neutron capture on ^{235}U whose products are ^{236}U and ^{237}U . ^{237}U (half - life = 6.75 days) finally decays to ^{237}Np . This reaction is preponderant in thermal reactors.



b) 90% of neptunium production in fast reactors is through (n,2n) reactions on ^{238}U [12] which only happens above ~ 6 MeV, i.e. for fast neutrons.

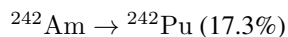
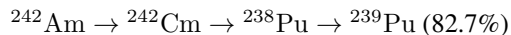
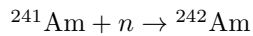


During irradiation process, neptunium either fissions or capture neutron to become ^{238}Np which is short lived with a half - life of 2.1 days. ^{238}Np decays to ^{238}Pu . The following reaction represents the transmutation steps of ^{237}Np :



^{238}Pu being a strong alpha emitter is highly thermally active. Nevertheless, when mixed with existing plutonium it can be utilized as fuel since it is a neutron provider in a fast spectrum [12].

Americium: Due to its significant production level and gamma activity, Americium is considered as the prime candidate for transmutation. It has relatively short half - life and the dominant isotope in the irradiated nuclear fuel is ^{241}Am . Nevertheless, smaller but significant quantities of ^{242}Am and ^{243}Am are also produced. ^{241}Am is produced from the decay of ^{241}Pu which has a half-life of 14.4 years. ^{241}Am is consumed by absorption rather than fission, and the main product in the process is ^{238}Pu , from the successive decays of ^{242}Am and ^{242}Cm . Further isotopes are also produced in small quantities [12]. The transmutation of ^{241}Am involves the following reactions:



Curium: This is a major contributor to neutron emissions. It also significantly contributes to the gamma activity and radiotoxicity. However, its transmutation is generally ruled out due to low fission and capture cross sections of its principal isotopes, ^{242}Cm and ^{244}Cm .

For these reasons, we consider ^{241}Am for transmutation studies that will be covered in section 6.1.

The thorium cycle produced less MA waste, as can be seen from the pathways in Figure 1. Absorption of a neutron moves one column to the right: beta decay moves one row down. Taking ^{241}Am as a typical MA isotope, the path starting at ^{238}U , as shown in Figure 1, is much shorter (6 steps rather than 14) than that from ^{233}Th . Furthermore the probability of neutron capture by ^{233}U is, at most energies, about a factor of 10 less than its fission probability, whereas for ^{239}Pu the comparable factor is smaller, in the range 2 to 3, as can be seen from the cross sections in the JEFF3.1N library [13].

1.4 Thorium ADSR studies

Thus thorium is a promising alternative to uranium fuel in an ADSR because of its properties: proliferation resistance, abundance in nature and nuclear waste management.

Rather than designing a new thorium filled reactor for the present investigations, we used the design of reactor MYRRHA. The Belgian nuclear research Centre SCK·CEN at Mol has proposed MYRRHA (Multipurpose hYbrid Research Reactor for High-tech Applications) [14] which is currently under development and considerable detailed design work has been

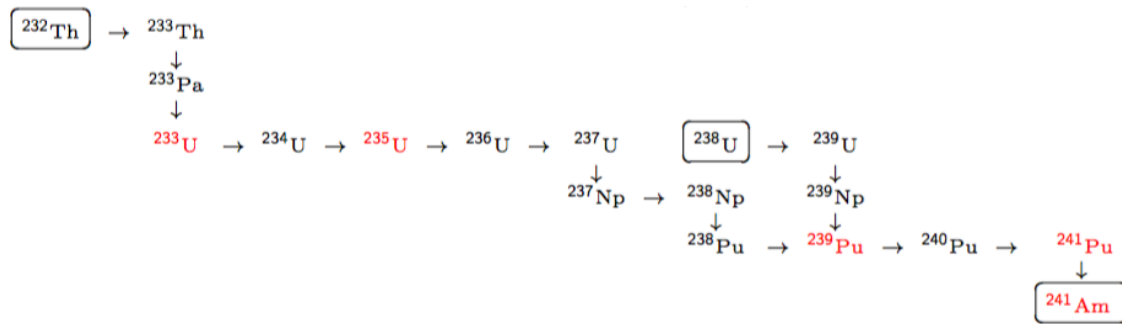


Figure 1: Minor actinides: principal pathways from ^{232}Th and ^{238}U .

done, though this does not include studies using thorium fuel. We have undertaken such simulations partly to increase our understanding of the possible uses of MYRRHA, and also to consider the problems of thorium fertile to fissile conversion and MA incineration using a mature and realistic ADSR design. The studies were done using two simulation programs: MCNPX and Geant4. Early versions of these results have been previously published[15, 16].

2 The MYRRHA Reactor

The MYRRHA reactor has been proposed to replace the Belgian Reactor 2 (BR2). It is a flexible design which can run either in critical or subcritical mode. It consists of an accelerator delivering a proton beam of 600 MeV in energy and about 4 mA beam current, and molten lead bismuth eutectic (LBE) as coolant which also acts as a spallation target and a subcritical core fueled with mixed oxide (MOX). It is now approved and under construction and due deliver its first beams in 2026.

The geometry and material composition of the core is described by an MCNPX file provided by the MYRRHA team [17] and shown in Figure 2. The cells shown in the above geometry are hexagonal cells with 10.45 cm between opposite

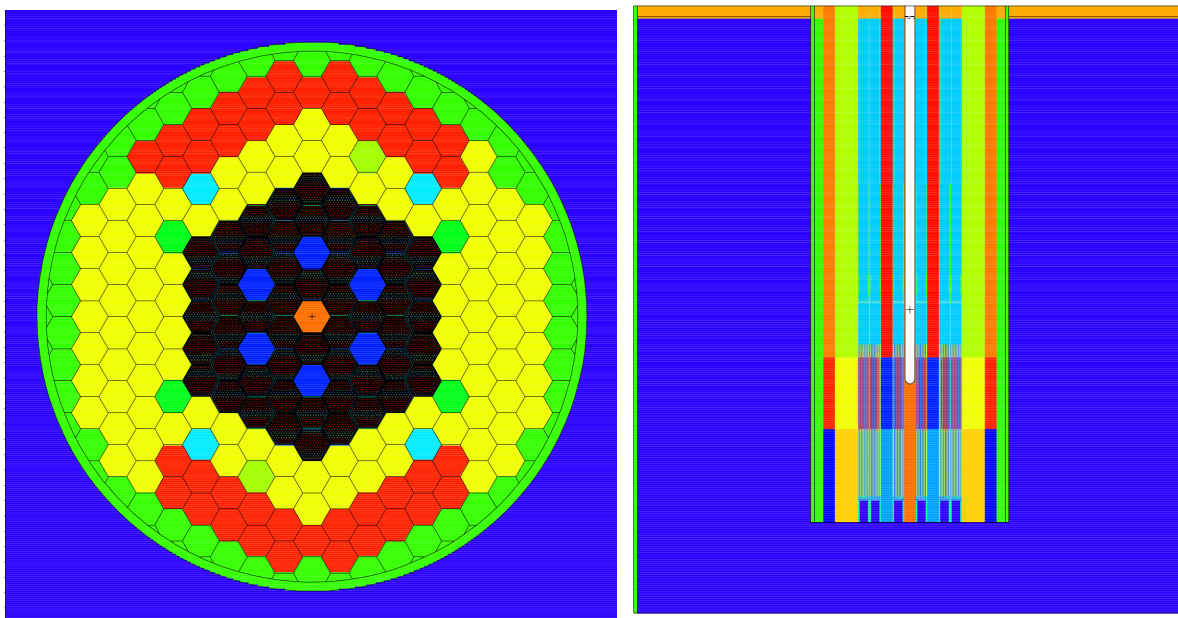


Figure 2: MCNPX visualization of the full reactor considering a horizontal section (left) and vertical section (right). Colours (available in the online version) are explained in the text.

faces. Longitudinally the rods are divided into three parts, with the height of central active part being 65 cm. It is helpful to divide the cells into:

1. Inner cells, also known as core. Six fuel assemblies (black) surround the spallation target (orange). The next hexagonal ring contains 12 cells, half of which are fuel assemblies and half are In-Pile Section (IPS) cells (deep blue) for material testing in high neutron fluxes. Fuel assemblies in the next two rings make up the total 54 such cells.
2. Outer cells (yellow), which mostly contain lead bismuth eutectic (LBE). The next ring out is made up of 26 of these and four cells (green) for control rods, not used in ADSR mode. The next ring is again LBE cells apart from two cells (yellow-green) intended for the production of Molybdenum isotopes and four cells (light blue) for Actinium. Rings after this also include Beryllium loaded reflectors (red) and finally stainless steel shielding (green).

2.1 Fuel mixtures

The following three fuel mixtures were used in the simulations, with compositions shown in Table 1 :

1. U/Pu mixture (Mix 1): Standard MYRRHA MOX fuel [17]. It consists of natural uranium plus plutonium (with a little americium) as obtained from fuel reprocessing. Oxygen is also included, as the fuel is used in the oxide form rather than being purely metallic.
2. Th/Pu mixture (Mix 2): All the uranium in Mix 1 is replaced by thorium, which naturally occurs as pure ^{232}Th . This represents a possible initial fuel mixture before any ^{232}Th to ^{233}U conversion has occurred.
3. Th/U mixture (Mix 3): All the Pu and Am in Mix 2 is replaced by ^{233}U . This represents an asymptotic fuel mix in which the initial MOX starter has been consumed, but has been replaced by ^{233}U produced from the ^{232}Th .

Fuel mix	Element	Percentage MCNPX	Percentage Geant4
Mix 1	^{16}O	11.6718	Same composition
	^{234}U	0.0033	
	^{235}U	0.4395	
	^{238}U	61.3717	
	^{238}Pu	0.6083	
	^{239}Pu	14.8343	
	^{240}Pu	7.0417	
	^{241}Pu	1.5924	
	^{242}Pu	2.0066	
	^{241}Am	0.4304	
Mix 2	^{16}O	11.6718	11.6718
	^{232}Th	58.4071	62.0000
	^{238}Pu	0.6865	0.6083
	^{239}Pu	16.7407	14.8343
	^{240}Pu	7.9467	7.0417
	^{241}Pu	1.7970	1.5924
	^{242}Pu	2.2645	2.0066
	^{241}Am	0.4857	0.4304
Mix 3	^{16}O	11.6718	11.6718
	^{232}Th	70.1260	59.8200
	^{233}U	18.2022	16.0000

Table 1: Compositions (percentages, by number) for the three different fuel mixes considered

Mix 1, the standard MYRRHA fuel mix, has a k_{eff} of 0.95178 ± 0.00059 as evaluated by the MCNPX KCODE process[1] (using 1000 cycles of 1000 particles, ignoring the initial 100 cycles). For mix 2, simply replacing all the uranium by thorium gives a very different k_{eff} , so the relative fractions of thorium and the fissile Pu/Am mix were adjusted to give a value approximately 0.95 - actually 0.94167 ± 0.00061 . This was used for the Geant4 studies. For the MCNPX studies a further slight adjustment brought k_{eff} to 0.95165 ± 0.00058 , much closer to the equivalent of mix 1.

A similar adjustment was made for mix3, the mixture used in Geant4 giving $k_{\text{eff}} = 0.96235 \pm 0.00061$ and the MCNPX mixture 0.95096 ± 0.00068 .

3 Simulation programs

3.1 MCNPX

MCNPX [1] is a well established program widely used in reactor simulations. Version 2.7.0 was used, with the standard ENDF/B-VII cross section libraries [18]. The geometry was specified by a input deck supplied to us by Edouard Malambu and Alexey Stankovsky of SCK·CEN, dated August 2014 [17] and taken from drawings and specifications version REV.1.6. The geometry shown in Figure 2 uses this deck. Various different configurations have been proposed in the past, but the configuration is now stable. Note in particular that the target occupies only a single cell, whereas in earlier designs it occupied several.

Each simulation was done using 10,000 initial protons and took typically 12 hours to run.

3.2 Geant4

Geant4 [2] is a program originally used to simulate particle physics detectors, but which has since been extended to many different fields. We used version 4.10.1, the latest release (December 2014) at the start of the study. The physics list QGSP_BIC_HP was used, based on earlier studies ([19], [20], [21]). 100,000 beam protons were used for the simulations. These protons are sufficient to provide statistically reliable results that can be compared with the results predicted by earlier studies [22, 15, 16].

3.2.1 Cross sections for transuranic elements

Because of its history, GEANT4 did not handle transuranic elements: the standard G4NDL library does not provide data for isotopes having atomic number $Z > 92$. However for reactor studies, such as this one, these cross sections are needed.

We therefore used the program of Mendoza et al [23, 24] to transform the widely used JEFF 3.1 library [13], which uses neutron cross sections from ENDF/B-VII and contains the relevant transuranic cross sections, into G4NDL format. Three environmental variables had to be specifically set:

- a) `G4NEUTRONHP_SKIP_MISSING_ISOTOPES=1`
- b) `G4NEUTRONHP_DO_NOT_ADJUST_FINAL_STATE=1`
- c) `AllowForHeavyElements=1`.

Even so there were problems: the program would run for several events and then crash with the message

```
Called G4PiNuclearCrossSection outside parametrization
```

or

```
***G4ElectroNuclearCrossSection::GetFunctions: A='<<244.064<<'(?). No CS returned!
```

Investigation showed that these messages were generated from code relating to the calculation of cross section formulae for pions and muons, which could not handle isotope nuclei with $Z > 92$. The 600 MeV beam energy is above the 289 MeV threshold energy for pion production, so pions and consequently muons are generated in our simulation, whereas others who have used Geant4 for conventional reactor studies where the energies do not exceed a few MeV will not have encountered this problem.

The relevant source code files were found to be `G4KokoulinMuonNuclearXS.cc`, `G4KokoulinMuonNuclearXS.hh` and `G4PiNuclearCrossSection.cc` and these were modified, after discussion with the Geant authors [25] to use $Z = 92$ in their formulae for nuclei with $Z > 92$.

While this is an approximation, it is a small effect that applies to a small number of targets and a very small number of particles. In all our fuel mixtures the fraction of transuranics is only a few percent, and the electromagnetic interaction of a pion with, say, one of the few americium nuclei is not going to be that different to its interaction with uranium. At 600 MeV and below the numbers of pions and muons are very small. An MCNPX study showed that for 10000 beam protons, 9,830,554 neutrons were produced, but only 438 charged pions are produced. A slight approximation to the behaviour of these 438 pions/muons is not going to affect the evaluated flux and energy spectrum of the neutrons. The overall effect on the results will be negligible.

There was also a warning produced - "### G4SeltzerBergerModel Warning: Majoranta exceeded! ", but it does not cause the program to crash and investigation showed it was not serious.

3.3 Implementation of the MYRRHA geometry in GEANT4

To implement the reactor geometry in GEANT4, a bottom-up approach was followed in which the fuel pin was considered as the smallest unit: pins are constructed with their gaps and cladding.

In the next step, fuel assemblies are created by arranging the pins in a hexagonal lattice. Different types of cells are also created such as the In Pile Section (IPS) cells and the spallation target.

These cells are then arranged in another lattice to build up the whole core. After the core, 5 outer rings are constructed including Lead bismuth eutectic (LBE) cells, Mo/Ac cells, control rods, reflectors and steel shielding cells.

GEANT4 has a variety of visualization drivers offering specific features to meet different demands of its users. In the present simulations, the OpenGL driver is used due to its fast visualization feature for demonstrating geometries, trajectories and hits [26, 27]. OpenGL offers interactive features: zoom, rotate and translate. However, for the complicated dimensions (Radial dimensions of a few millimeters and vertical dimensions of many centimeters) of the reactor, 'zoom' did not prove useful. Instead images were displayed with the radial dimensions enlarged temporarily for the purpose of better visualization. Such displays are shown below, and this system proved to be helpful in designing and debugging [28].

3.3.1 The Fuel pin

The fuel pin is a rod with cylindrical cladding loaded with cylindrical fuel pellets. Figure 3 shows the implementation of the fuel pin in GEANT4, with the original dimensions and in the enlarged version, for which the detail can be seen: it consists of three regions with 65 cm as length of the central active region, in which fuel (as described in section 2.1) is loaded. Dimensions are taken from the specifications provided by [17]. The structure of the fuel pellets is not simulated, the fuel is taken as being continuous in the rod. The upper and lower regions include insulator segments and a gas plenum chamber.

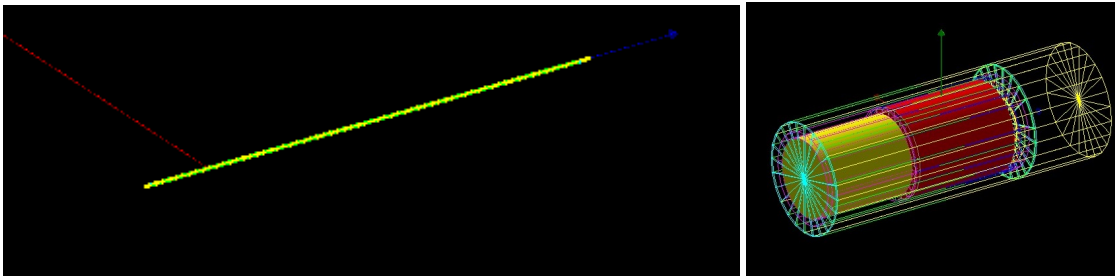


Figure 3: GEANT4 visualization of fuel pin: original dimensions (left) and enlarged dimensions (right)

3.3.2 Fuel assembly

Each fuel assembly is the collection of 91 fuel pins that are arranged in a hexagonal bundle. Figure 4 shows the steps in the creation of the fuel assembly from the fuel pin. In the enlarged picture (Complete FA), the blue and red cylindrical shape shows the upper and lower part of the fuel assembly respectively and the central region is the active part of the fuel assembly.

3.3.3 IPS cells

Six IPS cells are created and placed in the reactor core as shown in the Figure 5. Initially in the program the reactor core is created with all the fuel assemblies, then the designated locations are made empty and IPS cells are placed at these locations.

3.3.4 Central cell - the Spallation target

The Spallation target is one of the key component of the ADSR. The beam tube ends on hemispheric window as shown in Figure 6. The target is constructed using G4Tub shape for the beam tube and G4Sphere for the hemispherical end, with appropriate coordinates for the adjacent placement of these two sections of the target. The spallation target cell is then placed with the hemispheric end located at the center of the core.

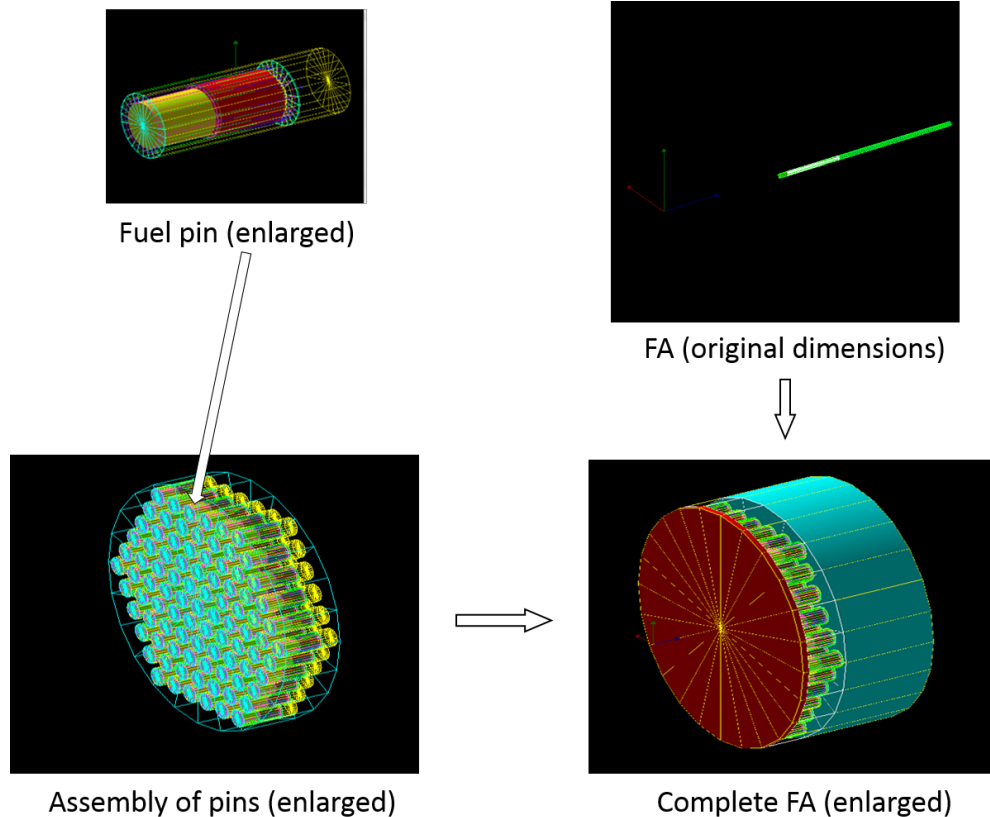


Figure 4: GEANT4 visualization of fuel assembly (FA)

3.3.5 The complete reactor

The inner cells include total 54 fuel assemblies and six IPS cells constituting the reactor core, as shown in Figure 7.

The outer cells are then added. These have the same dimensions but are filled with different materials for LBE cells, Mo-Ac cells, Beryllium reflectors and Stainless Steel shielding.

The complete picture of the reactor as modelled in GEANT4 with all the cells placed, is presented in Figure 8. It should be compared with the MCNPX model of Figure 2

4 Results: Neutron Fluxes and Energy Spectra

4.1 Neutron Flux

Average neutron fluxes were evaluated for the fuel cells, as this is important for fuel evolution, and for the three types of cell intended for irradiation: the IPS cells in the core and those for Molybdenum and Actinium production in the outer region. Neutrons of energy range 10^{-8} MeV to 100 MeV were considered. MCNPX results are obtained from the F4 neutron flux tally; for Geant4, the function G4PSPassageCellFlux is used to record the flux.

Values are shown in Table 2 for the 3 different fuel mixtures. Numbers shown are normalised to a nominal 1 mA proton beam current. Statistical errors are of order 5%. (The errors are calculated and printed for MCNPX: for Geant4 they were estimated by running the same job twice with a different random seed and examining the differences.)

The table shows that GEANT4 and MCNPX results are in fair agreement. There are differences, but there is no discernible general trend. It is not possible to assign causes to these differences - whether they are due to the details of the programs used, or the data libraries, or the slight difference in the value of k_{eff} , as described in Section 2.1, for Mixtures 2 and 3.

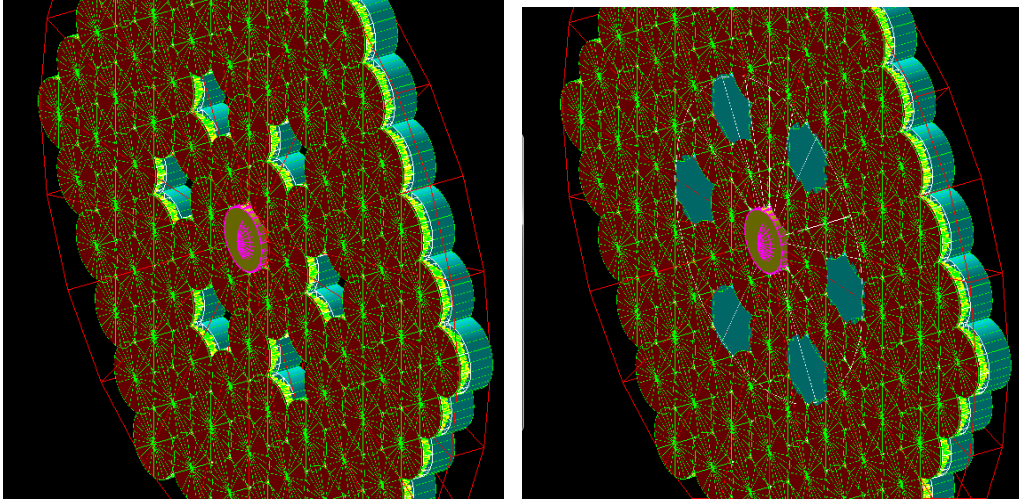


Figure 5: IPS assemblies: (left) empty locations for IPS (enlarged dimensions) and (right) IPS placed in the core

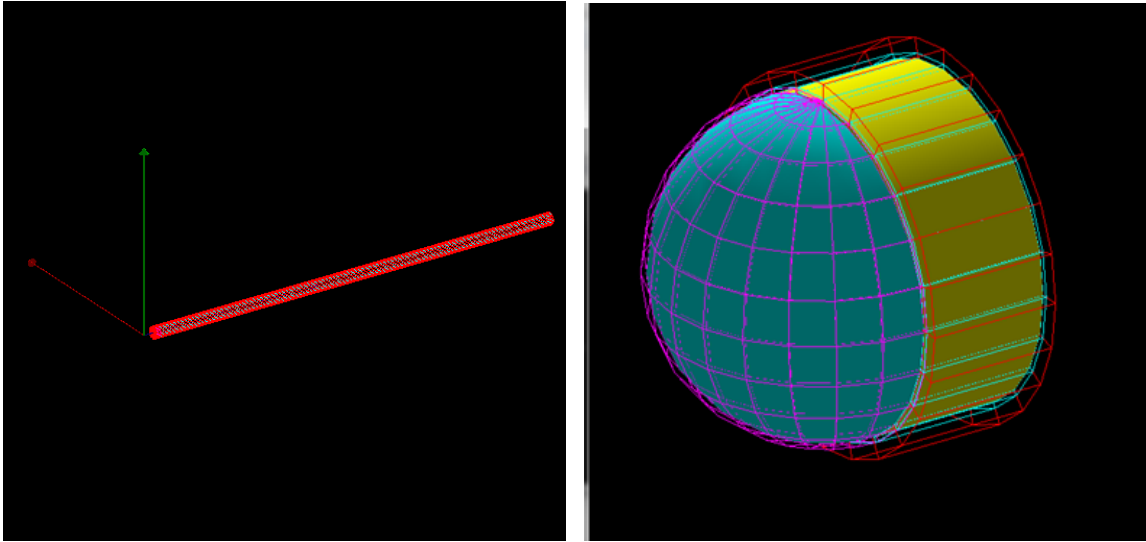


Figure 6: GEANT4 visualization of spallation target: Original (left) and Enlarged (right) dimensions

The simulations show similar fluxes for the inner IPS cells and the fuel cell average, with lower values for the Mo cells and even lower ones for the Ac cells further out. There are differences between the different fuel mixtures but no general trend can be discerned.

Location	Mix1		Mix2		Mix3	
	G4	MX	G4	MX	G4	MX
Fuel	6.28	7.08	6.37	5.80	8.62	8.41
IPS	5.19	8.48	8.76	6.98	8.34	9.95
Mo cell	2.8	4.8	5.07	3.91	6.94	6.04
Ac cell	1.17	1.09	0.93	0.90	1.98	1.37

Table 2: Average flux values (units are 10^{14} neutrons/cm²/s) for a 1 mA proton beam

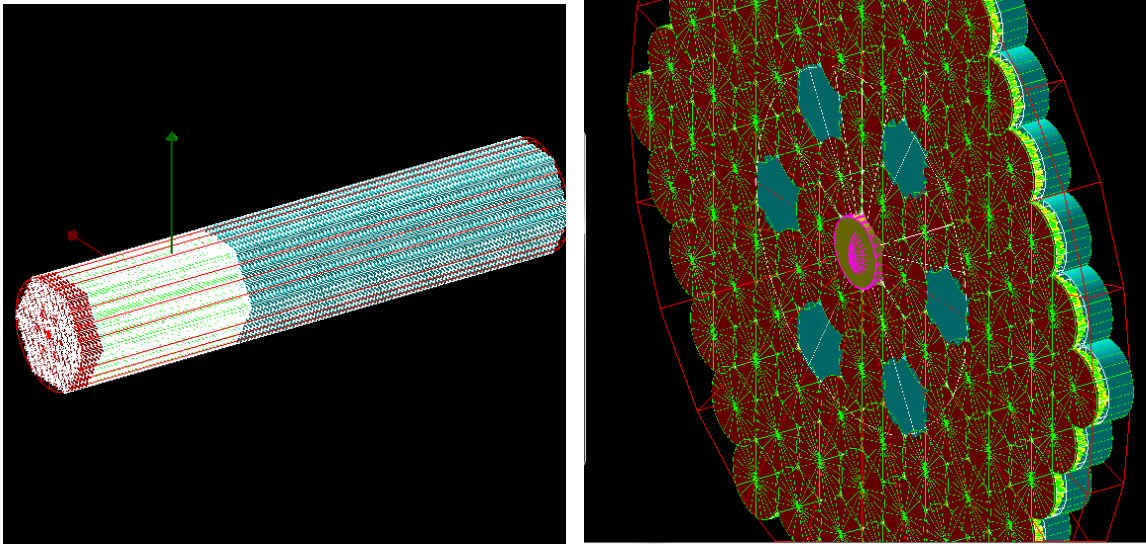


Figure 7: GEANT4 visualization of reactor core: Original dimensions (left) and enlarged dimensions (right)

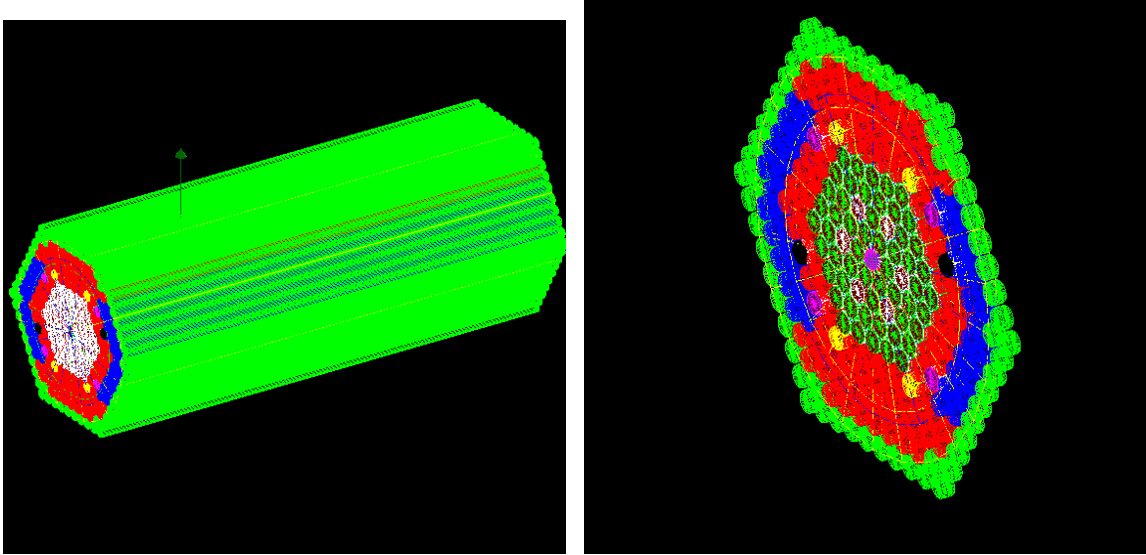


Figure 8: GEANT4 visualization of the reactor: (left) Original dimensions and (right) Enlarged Dimensions

4.2 Neutron energy spectra

We considered the energy spectra for the three fuel mixes as obtained by GEANT4 and MCNPX. The energy spectra for the fuel is presented in Figure 9 in terms of both energy and lethargy¹. The fuel cell spectra show a hard component – all the way up to the proton energy - though energies go all the way down to thermal energy. The spectra and the overall numbers agree well for GEANT4 and MCNPX. This is true for all the three fuel mixtures. Nevertheless they differ in detail: the most marked regions of disagreement being at low energies in the Fuel cells and at high energies in the IPS cells. Whether this is due to differences in the algorithms or in the data libraries is not clear, but detailed predictions involving these neutrons should be treated with appropriate caution. The fluctuations in the spectrum do not stem from low simulation statistics rather due to the energy dependence of the cross section. The results for the standard mixture are compatible with the earlier studies of Sarotto et al[22]

¹Lethargy is defined as the logarithm of the ratio of maximum energy that a neutron might have in a reactor to the neutron energy

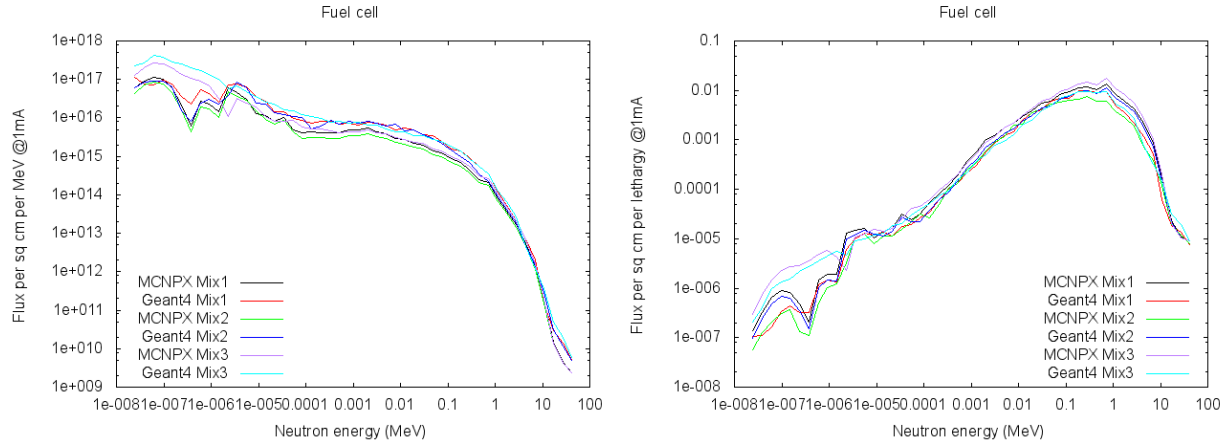


Figure 9: Neutron flux averaged over the fuel cells per unit energy(left) and lethargy (right)

Spectra of IPS regions shown in Figure 10 are taken as the average of 6 IPS cells spectra. Being ‘in pile’ they have neutron fluxes similar to those in the fuel cells that surround them but with fewer thermal neutrons.

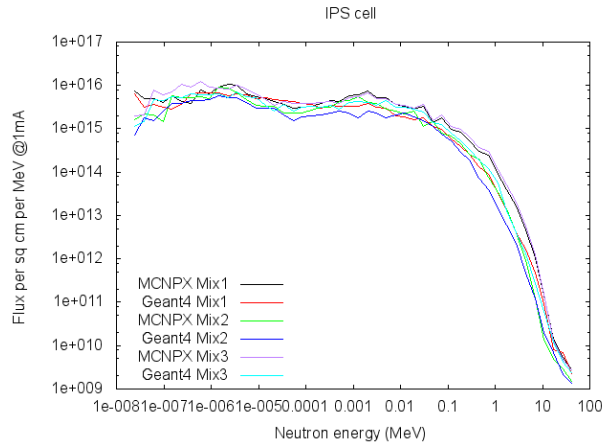


Figure 10: Neutron flux averaged over the IPS cells

The Mo and Ac production cells are farther away from the centre and the spectra, shown in Figure 11 in these regions are found to be softer, which is understandable as the neutrons reaching the outer cells have travelled further and undergone more collisions.

Energy distribution of the neutron flux can be divided into the following three regions [29]:

1. Thermal region - Neutron energy: 5×10^{-11} MeV to 5×10^{-7} MeV.
2. Epithermal region - Neutron energy: 5×10^{-7} MeV to 0.5 MeV.
3. Fast region - Neutron energy: 0.5 MeV to 20 MeV.

Based on this, the flux percentage for each considered region with respect to the integral flux and the ratio between the fast and the thermal components are presented in Table 3. The ratio depicts that the hardness of the spectra is 1% to 2% in IPS cells, 0.1% for fuel cells and much smaller in Mo Ac cells.

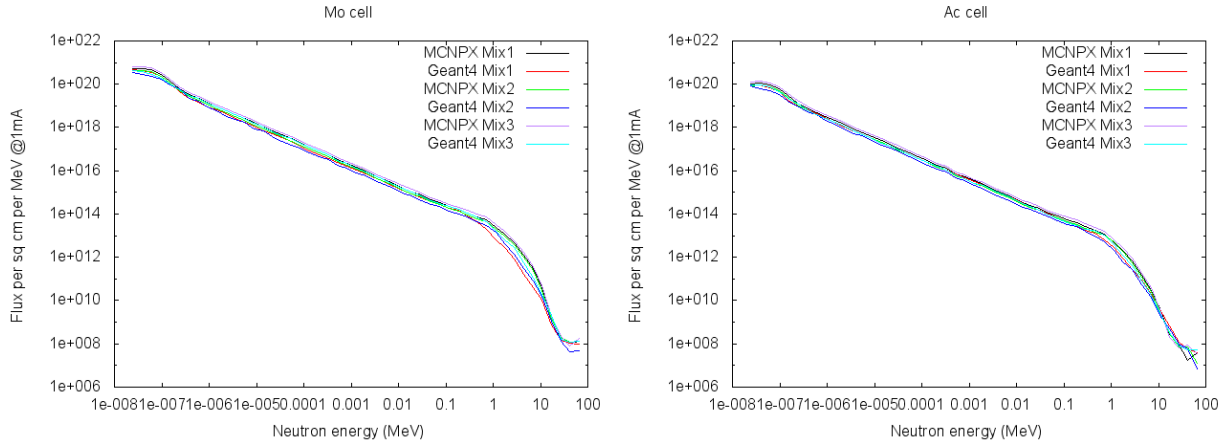


Figure 11: Neutron flux averaged over the Mo cells (left) and Ac cells (right)

Cell	Fuel	Program	Percentage			Ratio of fast to thermal
			Thermal	Epithermal	Fast	
Fuel	Mix1	MX	63.36	36.60	0.04	0.0007
		G4	53.17	46.78	0.05	0.0010
	Mix2	MX	61.25	38.70	0.04	0.0008
		G4	50.96	48.99	0.04	0.0008
	Mix3	MX	82.89	17.09	0.03	0.0003
		G4	77.68	22.30	0.02	0.0002
IPS	Mix1	MX	20.29	79.31	0.40	0.0195
		G4	21.48	78.33	0.20	0.0092
	Mix2	MX	18.61	81.12	0.26	0.0142
		G4	20.27	79.58	0.14	0.0071
	Mix3	MX	23.12	76.42	0.46	0.0197
		G4	21.23	78.48	0.29	0.0135
Mo	Mix1	MX	96.98	3.02	8.142×10^{-6}	8.396×10^{-8}
		G4	97.50	2.50	4.333×10^{-6}	4.443×10^{-8}
	Mix2	MX	96.99	3.01	8.297×10^{-6}	8.555×10^{-8}
		G4	96.80	3.20	7.417×10^{-6}	7.662×10^{-8}
	Mix3	MX	96.98	3.02	8.721×10^{-6}	8.992×10^{-8}
		G4	95.97	4.03	9.506×10^{-6}	9.905×10^{-8}
Ac	Mix1	MX	96.74	3.26	8.657×10^{-6}	8.949×10^{-8}
		G4	96.54	3.46	6.719×10^{-6}	6.960×10^{-8}
	Mix2	MX	96.77	3.23	9.117×10^{-6}	9.422×10^{-8}
		G4	96.39	3.61	6.406×10^{-6}	6.646×10^{-8}
	Mix3	MX	96.76	3.24	9.362×10^{-6}	9.674×10^{-8}
		G4	96.79	3.21	9.560×10^{-6}	9.877×10^{-8}

Table 3: Neutron flux percentage for different regions using GEANT4 and MCNPX for different fuel Mix

5 Results: Fuel evolution with thorium as fuel

5.1 Method

Fuel evolution takes place due to fission, α and β decay, and reactions with neutrons. So the number of atoms X of some isotope in an element of a nuclear reactor changes according to

$$\frac{dX}{dt} = Q_1Y + \lambda_2P - Q_3X - \lambda_4X \quad (1)$$

where Y is the number of atoms that can produce X by reacting with a neutron, and P is the number of atoms decaying to X at rate λ_2 , while X itself is absorbing neutrons (by (n,γ) or $(n,2n)$ or other reactions) at rate Q_3 and decaying at rate λ_4 . Q_1 is the creation reaction probability $\int \sigma_1(E)\phi(E)dE$ and Q_3 is the destruction probability $\int \sigma_3(E)\phi(E)dE$, where σ_1 and σ_3 are the relevant cross sections and ϕ is the flux; these terms involve different cross sections but the same neutron flux.

For a particular isotope not all of the terms in equation 1 may be relevant, however these four are the maximum we need to consider (they can be extended in cases where X is produced by more than one reaction, or as the product of more than one decay).

Equation 1 is a differential equation involving three unknowns: X , Y and P . Y and P will have similar equations of their own, and these may involve further species. To predict what will happen, a complete set of equations needs to be written, one for each isotope involved, known as the Bateman Equations.

Dropping the different names and calling the isotopes $X_1, X_2 \dots X_n$, or just \vec{X} there are n equations for the n isotopes. The equations have the simple matrix form:

$$\frac{d\vec{X}}{dt} = M\vec{X} \quad (2)$$

where M is a matrix, of which the elements are decay rates λ or reaction probabilities $\int \sigma(E)\phi(E)dE$.

These equations can be solved either by stepwise integration (Euler's method) or by an exact algebraic technique: the eigenvectors u_i and eigenvalues a_i of M are found (we use the R package `eigen`), the initial composition is expressed as a sum over u_i , $\vec{X}(0) = \sum_i C_i u_i$ and the mixture at time is then just $\vec{X}(t) = \sum_i C_i u_i e^{a_i t}$.

In Equation 1 and its generalisations the lifetime λ terms are taken from known data. The reaction Q terms depend on the neutron flux, convoluted with the appropriate cross section. In MCNPX these are provided on demand using 'Tally cards'. For Geant4 they had to be constructed by numerical integration of the flux obtained by the simulation program and the appropriate cross section as given by the JEFF3.1 library [13]. As these two sets of data did not generally use the same energy bins, interpolation was done using using the R function `approx`.

This solution uses the flux as determined above in section 4.2. Changes in the composition will lead to changes in the flux, so these calculations are not exact; nevertheless the changes are small and will not have a large effect on the results, so the approximation is accurate enough to be useful.

When the evolution $\vec{X}(t)$ is plotted then typically one sees the $e^{-\lambda t}$ decay of the components one starts with, and the rise and then fall, $e^{-\lambda t}(1 - e^{-\lambda' t})$ of the daughter products.

5.2 Fertile to Fissile conversion

Turning to the specific cases considered here, these involve the conversion of fertile isotopes to the intermediate nuclei through neutron capture events. For mix 1, this is the conversion of ^{238}U to ^{239}U while for mix 2 and mix 3 it is ^{232}Th to ^{233}Th . Rapid beta decay in both these cases leads to the formation of ^{239}Np and ^{233}Pa respectively. The half-life of ^{239}Np is 23 minutes and that of ^{233}Pa is 21 minutes, so these can be considered as instantaneous. The second beta decay transforms ^{239}Np to ^{239}Pu , which is still rapid with a half-life of 2.4 days, whereas for mix 2 and mix 3, conversion of ^{233}Pa to ^{233}U is relatively slower with a half-life of 27 days. Further, if ^{233}Pa absorbs a neutron in an intense neutron flux, it could lead to the process diverting in unwanted directions. This is an issue well known for thorium reactors [15].

GEANT4 and MCNPX calculated neutron flux convoluted with the cross section (as per equation 3) for the three relevant isotopes are presented in Table 4. The two programs GEANT4 and MCNPX agree that the conversion rates differ for the three fuel mixtures. As the composition changes, the probability of fertile to fissile thorium conversion increases. The protactinium absorption probabilities (indicating the loss of ^{233}Pa from the chain) are relatively large compared to the probabilities of thorium nuclei entering the chain, but the amount of ^{233}Pa in the fuel at any time is very small. The ^{233}Pa effect (neutron absorption in the intermediate state) can be evaluated by solving the Bateman equation over 230 days for 2.5 mA beam current. This is plotted in Figure 12. The effect is observed to be very small as ^{233}Pa stabilizes soon.

Fuel	U238		Th232		Pa233	
	G4	MX	G4	MX	G4	MX
U/Pu (Mix1)	0.026	0.028	0.034	0.045	0.075	0.18
Th/Pu (Mix2)	0.032	0.036	0.028	0.028	0.061	0.15
Th/U (Mix3)	0.035	0.046	0.035	0.039	0.076	0.19

Table 4: Neutron absorption rates for isotopes in the fuel cells for 1 mA beam

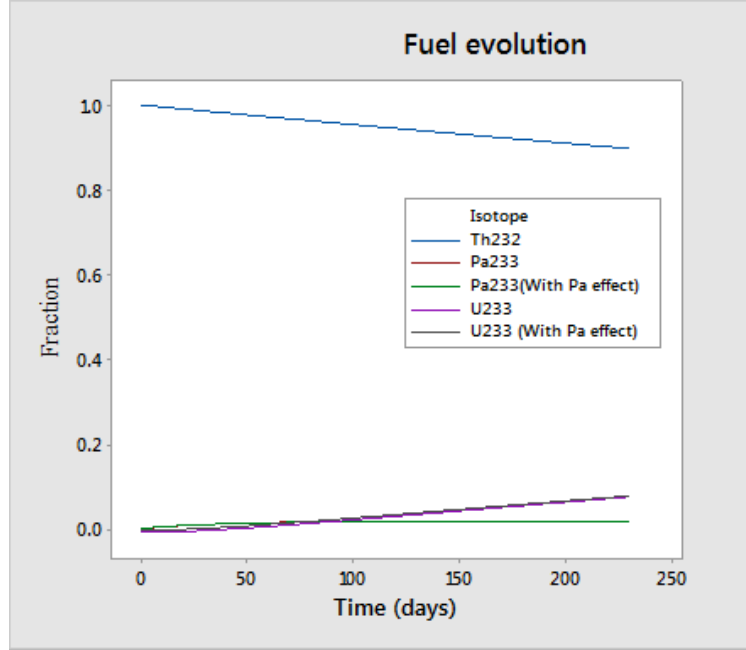


Figure 12: Thorium fuel evolution with and without ^{233}Pa neutron absorption effect

5.3 Production of ^{232}U

The isotope ^{232}U is important in the thorium cycle because it is inevitably co-produced with ^{233}U , and decays with the relatively short half live of 69 years, with a long decay chain involving high energy gamma rays [30] which can make handling in conventional glove boxes impossible, and can also damage electronics. This can be viewed as an advantage in that it makes weaponising fissile ^{233}U technically very difficult. It is, however, a possible problem in a thorium fuelled reactor.

There are 3 routes for its production, starting from isotopes already mentioned:

1. $^{233}\text{U} \xrightarrow{n, 2n} ^{232}\text{U}$
2. $^{233}\text{Pa} \xrightarrow{n, 2n} ^{232}\text{Pa} \xrightarrow{\beta^-} ^{232}\text{U}$
3. $^{232}\text{Th} \xrightarrow{n, 2n} ^{231}\text{Th} \xrightarrow{\beta^-} ^{231}\text{Pa} \xrightarrow{n, \gamma} ^{232}\text{Pa} \xrightarrow{\beta^-} ^{232}\text{U}$

The relevant production probabilities are shown in Table 5. The rate for the ^{231}Pa absorption is in good agreement between the two simulations (the MCNPX numbers quote a typical error of 1%) but for the $(n, 2n)$ probabilities there are differences. This was traced to the fact that these cross sections only become significant at high neutron energies (~ 10 MeV), at which point, as can be seeing from figure 9, the flux is falling rapidly. MCNPX uses the ‘tally’ feature to

Reaction	$^{233}\text{U}(n,2n) \ ^{232}\text{U}$	$^{233}\text{Pa}(n,2n) \ ^{232}\text{Pa}$	$^{232}\text{Th}(n,2n) \ ^{231}\text{Th}$	$^{231}\text{Pa}(n,\gamma) \ ^{232}\text{Pa}$
MCNPX	4.58×10^{-5}	1.74×10^{-4}	2.27×10^{-4}	1.41×10^{-1}
GEANT4	1.70×10^{-4}	4.33×10^{-4}	5.65×10^{-4}	1.44×10^{-1}

Table 5: Production probabilities for ^{233}U . The numbers in the table are as given by the MCNP tally, namely the flux in cm^{-2} multiplied by the cross section in barns.

record each individual track, weighted by the cross section whereas for Geant4 the neutron spectrum was histogrammed, and the production probabilities obtained by convoluting this with the tabulated energy-dependent cross section (taken from the ENDF70 library [18]). These tables are fine-grained at low energies with only a few values tabulated at high energies. For typical (n, γ) reactions this is adequate, but for these $(n, 2n)$ reactions the bin width is not narrow enough to describe the necessary detail. Hence the MCNPX numbers are used in the rest of this section.

The values in the tables are multiplied by 10^{-24} to be converted into a dimensionless number: the probability that a particular target nucleus will be converted in the specified way by a single beam proton. To find the total rate one multiplies by the density for a nominal 2.5 mA beam. These were put into the Bateman equations and the resulting time evolution is shown in figure 13

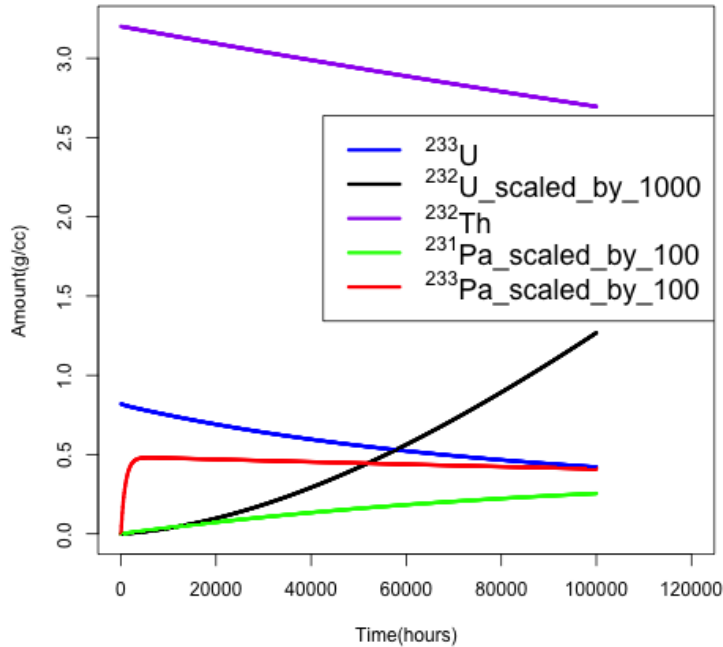


Figure 13: Evolution of a fuel rod, showing growth of ^{232}U

This considers fuel element evolving over a long period without replacement (100,000 hours is over 11 years). The intermediate ^{232}Pa and ^{231}Th decays, of the order of 1 day, are treated as instantaneous. It does not take into account changes in the flux due to fuel composition, or the accumulation of fission products, so it should be taken as indicative.

The largest contribution to ^{233}U growth comes from the ^{231}Pa . There is some contribution from the ^{233}U source, but the ^{233}Pa contribution is negligible.

A density of 1 mg/cc of ^{233}U , reached by the fuel after ~ 10 years, corresponds to an activity of 1.19 GBq/cc, which is well above the threshold for Intermediate Level Waste of 12 GBq/tonne. It will require careful handling and disposal.

6 Results: Incineration of Minor Actinides

From the neutron flux calculated in Section 4.2 the actinide burning rates in the reactor can be calculated. The absorption and fission cross sections, taken from the JEFF 3.1 library [13, 31] for different minor actinides are illustrated in Figure 14 .

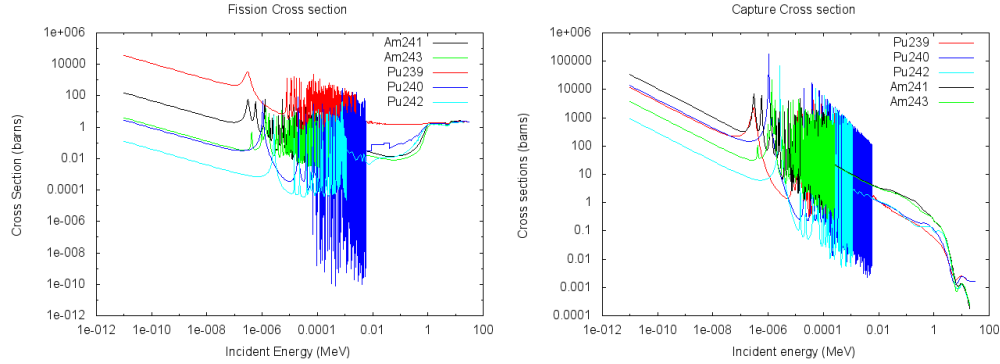


Figure 14: Fission and Absorption cross sections as functions of neutron energy, for various minor actinides, using the JEFF 3.1 library[13]

From these figures it can be seen that the fission cross section dominates over the absorption cross section above 1 MeV, demonstrating the advantage of fast neutrons for incineration. Such a hard neutron spectrum was observed in the fuel cell and IPS cells, in Figures 9 and 10. The spectra in the Mo and Ac cells in Figure 11 are not as hard as in the IPS and fuel cells but since these cells are available for irradiation, we also consider these locations for burn up studies.

The weighted flux F in a volume V is given by the convolution with the cross section

$$F = \frac{1}{V} \int_0^{E_{\max}} \phi(E) \sigma(E) dE \quad (3)$$

where V is in cm^3 , $\phi(E)$ is the total track length of the neutrons produced by a single beam particle, so $\phi(E)/V$ is the flux and $\sigma(E)$ is the reaction cross section (which needs to be multiplied by a factor 10^{-24} to convert barn to cm^2). F is thus [15] the probability that a given MA nucleus will be transformed in the neutrons produced by one beam particle. When multiplied by the beam current (in protons per second) this gives the burn-up rate: the inverse of the mean life time of the MA in the reactor.

This weighted flux is calculated by GEANT4 and MCNPX for a number of significant actinide species: ^{241}Am , ^{243}Am , ^{237}Np , ^{239}Pu , ^{240}Pu and ^{242}Pu for both the inner IPS cells and the outer cells used for Mo and Ac production (the two types are so similar they were combined). Three fuel mixtures described earlier are considered for these calculations. Results are shown in Table 6 and Table 7 respectively. The ratio in 7th and 8th column corresponds to the ratio of fission to absorption, according to the two programs. It tells whether fission or absorption is dominating.

The tables show that

1. Results of the two programs agree reasonably well: the difference shows the uncertainties inherent in such calculations.
2. Slightly higher burn up rates are predicted for Mix 3, according to MCNPX.
3. ^{239}Pu being important as a fuel rather than a waste product, is a special case. Its fission probability is higher than absorption, in the inner cells where the spectra are harder, as well as in the outer cells.
4. For the other isotopes in the table, the ratio of fission to absorption is respectable in the IPS cells but it is negligible in the outer cells. Exposing such isotopes in the inner IPS cell will either transmute them to short lived fission products and/or to some higher atomic weight nuclei through neutron absorption. The ratio in outer cells suggest limited use of these cells for incineration.

Isotope	Fuel	Inner IPS					
		Fission MX	Fission G4	Absorption MX	Absorption G4	Ratio MX	Ratio G4
²³⁹ Pu	U/Pu	0.23	0.12	0.04	0.02	5.57	4.92
	Th/Pu	0.19	0.24	0.03	0.04	5.82	5.64
	Th/U	0.27	0.16	0.05	0.03	6.09	4.73
²⁴⁰ Pu	U/Pu	0.06	0.02	0.04	0.02	1.49	1.00
	Th/Pu	0.06	0.07	0.03	0.05	1.62	1.43
	Th/U	0.06	0.04	0.05	0.03	1.15	1.19
²⁴² Pu	U/Pu	0.05	0.02	0.05	0.03	0.98	0.62
	Th/Pu	0.04	0.05	0.04	0.05	1.02	1.02
	Th/U	0.06	0.02	0.06	0.04	1.15	0.59
²⁴¹ Am	U/Pu	0.05	0.02	0.21	0.12	0.24	0.15
	Th/Pu	0.04	0.05	0.16	0.19	0.26	0.23
	Th/U	0.06	0.02	0.23	0.16	0.28	0.14
²⁴³ Am	U/Pu	0.04	0.01	0.20	0.12	0.18	0.11
	Th/Pu	0.03	0.03	0.15	0.18	0.20	0.17
	Th/U	0.05	0.02	0.21	0.15	0.21	0.10

Table 6: Neutron absorption rates for isotopes in the inner IPS cells using GEANT4 and MCNPX for 1 mA beam. Units are probability per beam proton times 10^{24} .

Isotope	Fuel	Outer Mo Ac cells					
		Fission MX	Fission G4	Absorption MX	Absorption G4	Ratio MX	Ratio G4
²³⁹ Pu	U/Pu	5.78	4.43	2.91	2.22	1.98	2.00
	Th/Pu	4.70	3.51	2.37	1.89	1.99	1.85
	Th/U	6.50	4.10	3.37	2.15	1.93	1.91
²⁴⁰ Pu	U/Pu	0.01	0.00	3.80	2.77	0.00	0.00
	Th/Pu	0.01	0.01	3.08	2.36	0.00	0.00
	Th/U	0.01	0.01	4.67	3.22	0.00	0.00
²⁴² Pu	U/Pu	0.01	0.00	0.26	0.19	0.03	0.01
	Th/Pu	0.01	0.00	0.21	0.15	0.03	0.02
	Th/U	0.01	0.01	0.32	0.23	0.03	0.02
²⁴¹ Am	U/Pu	0.06	0.04	7.86	5.77	0.01	0.01
	Th/Pu	0.05	0.04	6.36	5.43	0.01	0.01
	Th/U	0.07	0.05	9.18	6.57	0.01	0.01
²⁴³ Am	U/Pu	0.01	0.00	2.04	1.50	0.00	0.00
	Th/Pu	0.01	0.00	1.66	1.26	0.00	0.00
	Th/U	0.01	0.01	2.51	1.86	0.00	0.00

Table 7: Neutron absorption rates for isotopes in the outer Mo Ac cells using Geant4 and MCNPX for 1 mA beam. Units are probability per beam proton times 10^{24} .

6.1 Americium incineration

The incineration of ²⁴¹Am in the IPS cell with Mix2 using GEANT4 and MCNPX, based on these burn up rates, is shown in Figure 15. The deviations, shown in Figure 16, are typically a few percent. The Bateman equations were solved over the period of 23 years by eigenvalue method described in section 5.1. The reaction rates, the Q factors in equation 1, are obtained from the tables and the decay rates are the inverse of the lifetimes of the isotopes. Single absorption and subsequent decays are considered. As discussed in subsection 1.3, ²⁴¹Am is consumed by absorption rather than fission. ²³⁸Pu is the main product in this process which is produced from the successive decays of ²⁴²Am and ²⁴²Cm. Other isotopes are also produced in smaller quantities.

These solutions are indicative in that they assume continuous operation of the reactor, and they ignore changes in the composition of the fuel (including the accumulation of fission products). To include such efforts would require many assumptions about the duty cycle and fuel processing strategy, and would not effect the overall conclusions. This shows

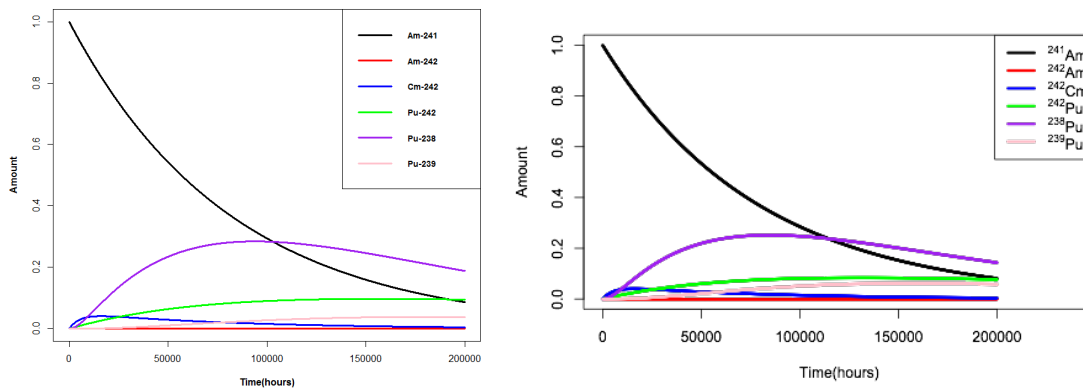


Figure 15: Evolution of ^{241}Am and its products: GEANT4 (Left) and MCNPX (Right)

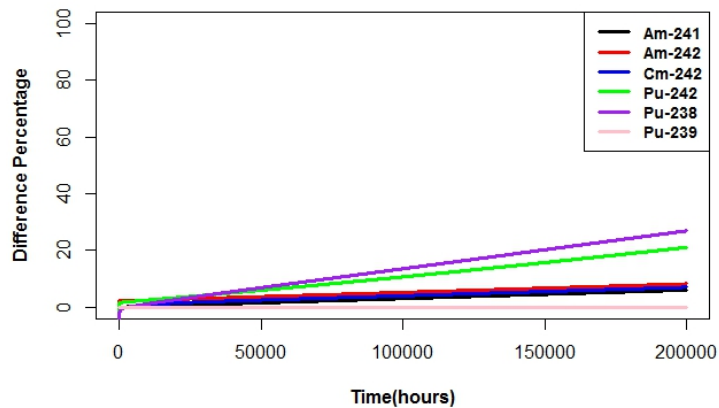


Figure 16: Evolution of ^{241}Am and its products: percent difference between GEANT4 and MCNPX

that the typical minor actinide ^{241}Am would be incinerated in MYRRHA. There would be small quantities of other isotopes produced but they present less of a problem as regards storage. However the process would be slow. An economically effective ^{241}Am burner would need to operate at much higher currents. However, the MYRRHA reactor would be a useful prototype.

6.2 Minor actinide production and net incineration

In order to compare the incineration capability of uranium and thorium based fuel, it is important to investigate the net incineration in the two fuel cycles. The amount of minor actinide produced is compared with that incinerated, as calculated in subsection 6.1. In the same model the formation of ^{241}Am starting from uranium or thorium is considered, using GEANT4 and MCNPX. The assumptions made in this modelling are:

1. Short life time decays are considered spontaneous.
2. Accelerator operation at 2.5 mA is continuous.
3. The entire fuel is treated as a single lumped object.
4. Variation in the neutron spectrum during fuel evolution is neglected.
5. A nominal timescale of 100 years.

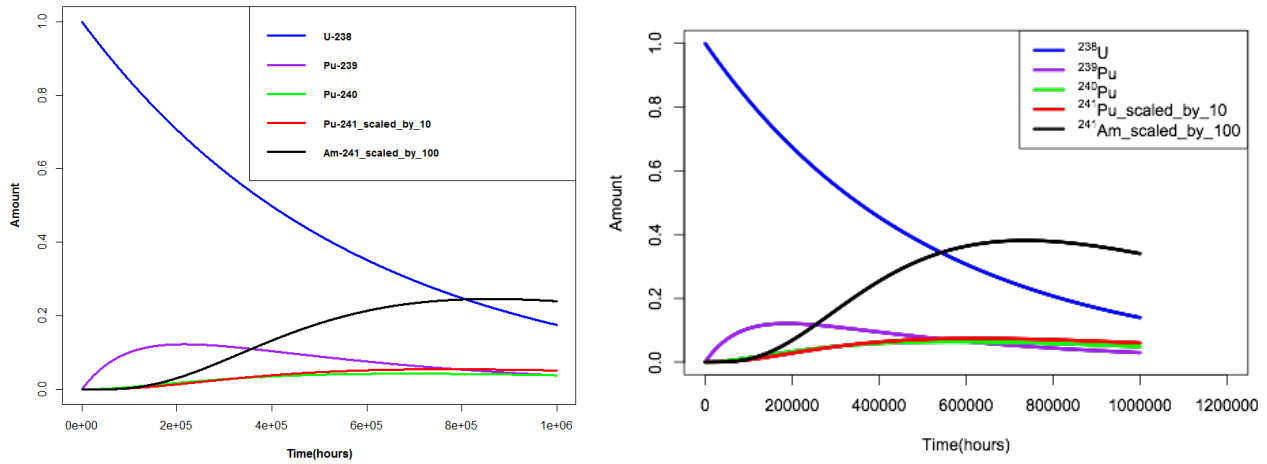


Figure 17: Evolution for ^{238}U and its products, Geant4 (Left) and MCNPX (Right)

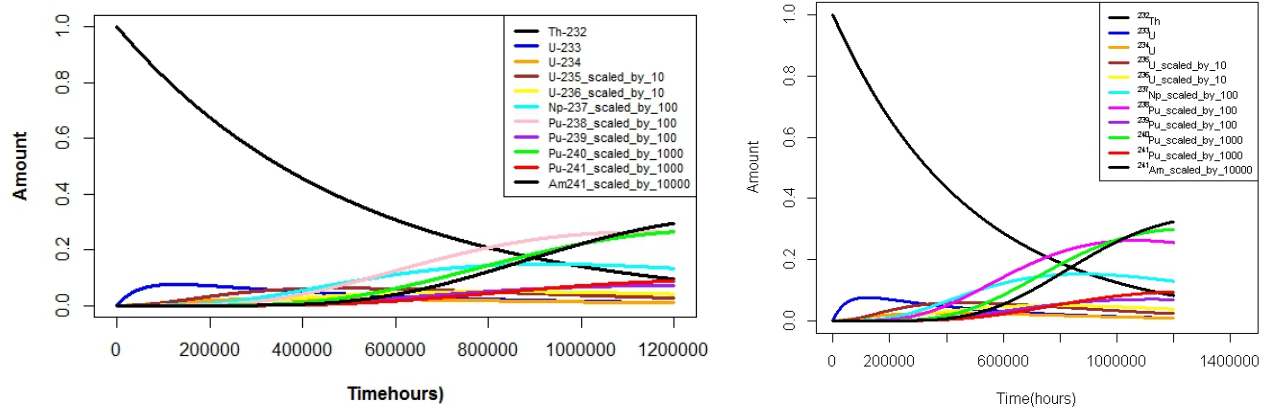


Figure 18: Evolution for ^{232}Th and its products, GEANT4 (Left) and MCNPX (Right)

Results of GEANT4 and MCNPX for uranium and thorium fuel cycles are shown in Figure 17 and 18. From the figures, it is clear that both the codes agree well for the trends in the two fuel cycles. It can be noted from Figure 17 that the amount of ^{241}Am produced from a Uranium base needs to be scaled by factor of ~ 100 to be visible. So $\sim 0.4\%$ of ^{238}U transforms into ^{241}Am and although this is a small fraction, given the large amount of ^{238}U in the fuel, it is producing a significant amount of ^{241}Am . On the other hand, ^{241}Am production from thorium (Figure 18) needs scaling by a factor of 10000 to be visible. Minor actinide production is decreased by a factor of ~ 100 when using thorium based in place of uranium based fuels.

7 Conclusions and future work

1. The reactor geometry has been successfully implemented using GEANT4.
2. The neutron flux spectra obtained by different simulation programs GEANT4 and MCNPX are benchmarked against each other and show good agreement for neutron flux spectra at various location of the reactor. The fuel spectra by these two programs also agree with other studies ([22]).

3. However there are some differences in the predictions, for some quantities in some regions, showing the usefulness of having two simulation programs to point out where predictions can be less reliable.
4. Broad features of neutron spectra are same for the three fuel mixes at all the chosen locations of the reactor. This indicates that provided the reactivity remains the same (in this case $K_{\text{eff}} = 0.95$), the spectra is insensitive to different fuel composition. Nevertheless they differ in detail which could be due to different absorption cross sections of the isotopes.
5. GEANT4 and MCNPX results presented in Table 6 and Table 7 depict that MYRRHA can convert measurable amount of minor actinide waste hereby proving the concept of industrial transmutation system.
6. Net incineration in case of ^{241}Am is improved with thorium fuels as the amount of ^{241}Am produced is much smaller than the amount incinerated.
7. The spectrum is harder and greater near the centre of the reactor. While the fuel cells are full (with fuel) there is space in the IPS that can be used for incineration studies.
8. The slow timescale in the study shows that long term waste problem is not going to be solved by MYRRHA itself, however it can be utilized as a demonstrator and a prototype for large scale systems that operate at much higher currents.

It is suggested to look at the fission products and burn up using the codes such as FISPACT or ALEPH to make time dependence more meaningful. But it will require detailed assumptions about the operational cycles and refuelling which were beyond the scope of this work.

Acknowledgements

The authors would like to thank the staff of MYRRHA, especially Hamid Aït Abderrahim, Edouard Malumbo and Gert van den Eynde, for providing data and for their comments and support.

References

- [1] Laurie S. Waters. MCNPX users' manual version 2.3.0. Technical report, LANL, LA-UR-02-2607, 2002.
- [2] S. Agostinelli et al. Geant 4 - a simulation toolkit. *Nucl. Instrum & Meth. A*, 506:250, 2003.
- [3] CD Bowman, ED Arthur, PW Lisowski, GP Lawrence, RJ Jensen, JL Anderson, B Blind, M Cappiello, JW Davidson, TR England, et al. Nuclear energy generation and waste transmutation using an accelerator-driven intense thermal neutron source. *Nuclear Instruments and Methods in Physics Research Section A: Accelerators, Spectrometers, Detectors and Associated Equipment*, 320(1-2):336–367, 1992.
- [4] F Carminati et al. Report cern-at-93-47 (et). Technical report, CERN/LHC/96-01 (EET), 1993.
- [5] H Nifenecker, S David, JM Loiseaux, and O Meplan. Basics of accelerator driven subcritical reactors. *Nuclear Instruments and Methods in Physics Research Section A: Accelerators, Spectrometers, Detectors and Associated Equipment*, 463(3):428–467, 2001.
- [6] Hervé Nifenecker, Olivier Meplan, and Sylvain David. *Accelerator driven subcritical reactors*. CRC Press, 2003.
- [7] H Ait Abderrahim, V Sobolev, E Malambu, et al. Fuel design for the experimental ADS MYRRHA. In *Technical Meeting on use of LEU in ADS. IAEA, (Vienna, Austria, 2005)*, pages 1–13, 2005.
- [8] Sara Changizi. Neutronic analysis of the multipurpose hybrid research reactor for high-tech applications (MYRRHA) with a monte carlo code serpent, 2012.
- [9] Yoshihiro Ishi, M Inoue, Y Kuriyama, Y Mori, T Uesugi, JB Lagrange, T Planche, M Takashima, E Yamakawa, H Imazu, et al. Present status and future of FFAGs at KURRI and the first ADSR experiment. *Proc. of IPAC10, Kyoto*, page 1323, 2010.
- [10] Thorium fuel cycle — potential benefits and challenges. https://www-pub.iaea.org/mtcd/publications/pdf/te_1450_web.pdf. Accessed 18.12.2018.
- [11] Graham Fairhall. Transmutation position paper. National Nuclear Laboratory, 2019.
- [12] Timothee Kooyman, Laurent Buiron, and Gerald Rimpault. A comparison of curium, neptunium and americium transmutation feasibility. *Annals of Nuclear Energy*, 112:748–758, 2018.
- [13] Jeff-3.1 evaluated data library. https://www.oecd-nea.org/dbforms/data/eva/evatapes/jeff_31/. Accessed: 22 September 2019.

- [14] MYRRHA: An innovative research installation. http://sckcen.be/en/Technology_future/MYRRHA. Accessed 18.12.2018.
- [15] Roger Barlow, James Burlison, Tristan Edwards, Alisa Healy, Alex Masterson, Hamid Ait Abderrahim, Edouard Malambu, and Gert van den Eynde. Studies of MYRRHA using thorium fuel. *International Journal of Hydrogen Energy*, 41(17):7175–7180, 2016.
- [16] Roger Barlow and Asiya Rummana. Actinide incineration with thorium fuel: A STUDY USING THE MYRRHA DESIGN. In *Proceedings of International Meeting on Nuclear Applications for Accelerators (AccApp'17)*. July 31-August4, 2017 (pp. 268-278). Quebec, Canada, 2017.
- [17] Edouard Malambou and Stankovskiy A. Description based on MYRRHA rev 1.6, 2014.
- [18] Chadwick M B et al. ENDF/B-VII.0: Next generation evaluated nuclear data library for nuclear science and technology. *Nucl. Data Sheets*, 107:2931, 2006.
- [19] Roger Barlow and Asiya Rummana. Simulations of spallation neutron distributions. In *Proceedings of International Meeting on Nuclear Applications for Accelerators (AccApp'15)*. November 10-13, 2015 (pp. 312-317). Washington, DC, 2015.
- [20] Roger Barlow, Asiya Rummana, and Rebecca Seviour. Characterisation of the spectra of spallation neutron sources through modelling. In *Proceedings of International particle accelerator conference (IPAC'16)*. May 8-13, 2016 (pp. 1950-1952). JACOW, Geneva, Switzerland, 2016.
- [21] Asiya Rummana and R Barlow. Simulation and parameterisation of spallation neutron distributions. In *Proceedings of the 4th Workshop on ADS and thorium (ADST2016)*. 31 August-2 September 2016. University of Huddersfield, England. Online at <http://pos.sissa.it/cgi-bin/reader/conf.cgi?confid=279>, id. 23, 2016.
- [22] Massimo Sarotto, Diego Castelliti, Rafael Fernandez, Damien Lamberts, Edouard Malambu, Alexey Stankovskiy, Wadim Jaeger, Marco Ottolini, Francisco Martin-Fuertes, Laurent Sabathé, et al. The MYRRHA-FASTEF cores design for critical and sub-critical operational modes (eu fp7 central design team project). *Nuclear Engineering and Design*, 265:184–200, 2013.
- [23] E Mendoza, D Cano-Ott, C Guerrero, and R Capote. New evaluated neutron cross section libraries for the Geant4 code. Technical report, International Atomic Energy Agency, 2012.
- [24] Emilio Mendoza, Daniel Cano-Ott, Tatsumi Koi, and Carlos Guerrero. New standard evaluated neutron cross section libraries for the GEANT4 code and first verification. *IEEE Transactions on Nuclear Science*, 61(4):2357–2364, 2014.
- [25] Alberto Ribon. Private communication, 2018.
- [26] Detector Simulation Visualisation. <https://indico.cern.ch/event/294651/sessions/55918/attachments/552022/760637/Visualisation.pdf>. Accessed 25.12.2018.
- [27] John Allison, Laurent Garnier, Akinori Kimura, and Joseph Perl. The Geant4 Visualization System — A Multi-Driver Graphics System. *International Journal of Modeling, Simulation, and Scientific Computing*, 4(supp01):1340001, 2013.
- [28] Asiya Rummana. *Spallation Neutron Source for an Accelerator Driven Subcritical Reactor*. PhD thesis, University of Huddersfield, 2019.
- [29] F Molina, P Aguilera, J Romero-Barrientos, HF Arellano, J Agramunt, J Medel, JR Morales, and M Zambra. Energy distribution of the neutron flux measurements at the chilean reactor rech-1 using multi-foil neutron activation and the expectation maximization unfolding algorithm. *Applied Radiation and Isotopes*, 129:28–34, 2017.
- [30] Jungmin Kang and Frank von Hippel. U-232 and the proliferation- resistance of u-233 in spent fuel. *Science & Global Security*, 9:1, 2001.
- [31] Geant4 library. <https://www-nds.iaea.org/geant4/libraries/JEFF31N/>. Accessed: 09.09.2021.